



Universidad Autónoma
de Madrid

Biblos-e Archivo
Repositorio Institucional UAM

Repositorio Institucional de la Universidad Autónoma de Madrid

<https://repositorio.uam.es>

Esta es la **versión de autor** del artículo publicado en:
This is an **author produced version** of a paper published in:

Particle and Particle Systems Characterization 36.91 (2019): 1900233

DOI: <https://doi.org/10.1002/ppsc.201900233>

Copyright: © 2019 WILEY-VCH Verlag GmbH & Co. KGaA, Weinheim

El acceso a la versión del editor puede requerir la suscripción del recurso

Access to the published version may require subscription

DOI: 10.1002/ ((please add manuscript number))

Article type: Full Paper

Real-Time Operation of Photovoltaic Optoelectronic Tweezers: New Strategies for Massive Nanoobject Manipulation and Reconfigurable Patterning

*Carlos Sebastián-Vicente, Esmeralda Muñoz-Cortés, Angel García-Cabañes, Fernando Agulló-López, and Mercedes Carrascosa**

C. Sebastián-Vicente, E. Muñoz-Cortés, Dr. A. García-Cabañes, Prof. F. Agulló-López, Prof. M. Carrascosa

Departamento de Física de Materiales, Universidad Autónoma de Madrid, c/ Francisco Tomás y Valiente 7, 28049 Madrid, Spain

E-mail: m.carrascosa@uam.es

Prof. F. Agulló-López, Prof. M. Carrascosa

Instituto de Ciencia de Materiales Nicolás Cabrera, Universidad Autónoma de Madrid, 28049 Madrid, Spain

Keywords: optical manipulation, optoelectronic tweezers, nanoparticle structures, bulk photovoltaic effect, ferroelectric materials

Optical and optoelectronic techniques for micro- and nano-object manipulation are becoming essential tools in nano- and biotechnology. Among optoelectronic manipulation platforms, photovoltaic optoelectronic tweezers (PVOT) are an emergent technique particularly successful producing permanent nanoparticle microstructures. In this work, new strategies to enhance the capabilities of PVOT, based on real-time operation, are investigated. This optoelectronic platform uses z-cut LiNbO₃:Fe substrates under excitation by a Gaussian light beam. Unexpected results show that during illumination, metallic particles previously deposited on the substrate are ejected from the light spot region. This behavior differs from the trapping phenomenon observed in previous work on PVOT operation, using a sequential method in which illumination is previous to particle manipulation. To discuss the results a novel mechanism of charge exchange between particles and the ferroelectric substrate is proposed. Applications of this repulsion behavior are investigated. On the one hand, either particle repulsion or trapping in the illuminated region can be obtained by simply light switching on/off. On the other hand, by moving the light spot, different kinds of arbitrarily

shaped tracks empty or filled with particles along the light path are obtained. The results demonstrate key new capabilities of PVOT such as pattern drawing, erasure and reconfiguration.

1. Introduction

The manipulation and trapping of micro and nano-objects, such as molecules, cells or bacteria and micro and nanoparticles (NPs) is a matter of increasing relevance for a variety of applications in photonics, optofluidics, nanotechnology and bio-technology.^[1–4] First approaches include conventional optical tweezers^[5,6] and electrokinetic methods,^[7] which have undergone lately an overwhelming development.^[4,8,9] More recently, new emerging tools based on optoelectronic platforms have been proposed^[10] and developed.^[11–13] They are particularly suitable for massive particle manipulation and can provide stronger manipulation forces than conventional optical tweezers.^[13,14]

Among optoelectronic techniques, particular attention has been recently attracted to the so called photovoltaic optoelectronic tweezers (PVOT) based on the bulk photovoltaic effect (PVE) presented by certain ferroelectrics.^[14–17] It allows generating high light-induced electric fields ($100\text{--}200\text{ kV cm}^{-1}$ ^[18]) in the ferroelectric substrate and so, particularly strong electrokinetic forces even larger than for other optoelectronic tweezers (OET).^[14] Moreover, in contrast to conventional OET, no external voltage supplier or electrodes are necessary because photoconduction appears without any externally applied electric field. Besides, only for PVOT, the PV fields and so, the trapping forces, remain after switching off the exciting light. This property makes PVOT very well suited to produce micro- and nano-particle stable patterns. In fact, the fabrication of patterns with a very large number of metallic or dielectric particles distributed over a relatively large area, more than 1000×1000 micrometers has been already reported^[19] and a variety of applications in different fields, such as photonics,^[19] nano-technology,^[20–23] biotechnology^[24–26] and optofluidics,^[27–29] have been recently

proposed and tested. PVOT manipulation involves not only the electrical response of the particles but also the singular optoelectronic (photorefractive) behavior of the ferroelectric substrate.^[30,31] Therefore, it presents more complexity but also opens new possibilities for controlling the trapping and manipulation process. Regarding the ferroelectric substrate, an alternative interesting manipulation method based in the thermally-induced electric fields generated in undoped lithium niobate has been also proposed and extensively developed.^[32,33,34,35] Moreover, the synergy between both processes has been also exploited.^[36] The pyroelectric method is clearly advantageous when needing very high electric fields because pyroelectric fields can reach values significantly higher than photovoltaic ones. In turn, the main advantage of PVOT is the high flexibility and spatial control provided by the illumination in order to generate arbitrary particle patterns. The present state of the art for PVOT has been summarized in a very recent review paper,^[37] whereas applications in biology and biotechnology have been reviewed by Blázquez-Castro et al..^[38]

Most PVOT experiments reported so far have used a two-step procedure usually called sequential method. First, light induces PV fields in the ferroelectric substrate. Then, once illumination is removed, particles approaching the substrate become trapped under the action of the PV field that remains in the dark. A simultaneous method with real-time particle manipulation during illumination is also possible although it has been scarcely investigated yet and so, many of its potentialities are still unexplored. Only a few experiments have been reported ^[26,39,40] by using a particular substrate configuration (crystals with the polar axis parallel to the surface, i.e. *x*- or *y*-cut samples) and only under sinusoidal illumination. In particular, results are available neither for real-time operation with *z*-cut crystals, a key configuration for two-dimensional operation,^[20,41] nor under Gaussian beam illumination. The particle dynamics is expected to be especially rich since it involves several competing

processes such as the generation of the PV field as well as the approach of the particles to the surface and their interaction with the ferroelectric substrate.

The main objective of the work is to investigate these new scenarios involving real-time operation under static or moving illumination on z-cut $\text{LiNbO}_3\text{:Fe}$ substrates. These substrates are particularly suitable because its active surface presents an axially-symmetric PV field pattern which has been recently simulated.^[42,43] Different situations of practical interest are investigated by studying in real time the dynamical response of the manipulation process: 1) real-time action on particles for static laser beam illumination, 2) response to moving light beams and 3) response to arbitrary combinations of light and dark intervals. A discussion on the capabilities offered by the novel strategies as well as on the involved physical mechanisms will be also provided. The results have put forward the complexity of the trapping process and have revealed the key role of the electron dynamics in the substrate. Specifically, a charge-exchange process is proposed between the particles and the substrate which offers a broad range of possibilities for particle control and manipulation. In particular, it provides an effective route for pattern erasure and reconfiguration. The results stand out the larger versatility of PVOT and the diversity of new scenarios where this tool can be applied.

2. Physical Basis of PVOT

The physical basis of the PV method has been reviewed in several recent papers.^[17,37] Before dealing with the dynamic processes concerning PVOT, we summarize here the main physical concepts affecting their operation.

The PVE^[17,44] appears in certain doped ferroelectrics and other non-centrosymmetric dielectrics, and it is singularly strong in Fe-doped LiNbO_3 , the crystal used in this work as PV substrate. The iron impurities appear in two valence states, Fe^{2+} and Fe^{3+} , which act as electron donors and acceptors, respectively. The PV effect arises from asymmetric photo-excitation of electrons from donor impurities (Fe^{2+}) that, due to the non-centrosymmetric

crystal lattice, gives rise to an electric PV current along the polar c -axis. The PV current density induced by an illumination of intensity I can be written as:

$$j_{pv} = es\phi l_{pv}[\text{Fe}^{2+}] \quad (1)$$

where e is the electron charge, s the photoionization cross section, $\phi = I/h\nu$ the photon flux, l_{pv} the PV effective drift length ($\approx 1\text{-}5 \text{ \AA}$) and $[\text{Fe}^{2+}]$ the concentration of donors.

Two crystal configurations are commonly used for the orientation of the ferroelectric polar axis (c -axis):^[41] parallel configuration, for which the polar axis is parallel to the active substrate faces (x - and y -cuts), and perpendicular configuration, with the polar axis normal to the active faces (z -cut). For the latter configuration, employed in this paper, the charge density generated by the PV current is induced essentially at the active surfaces whereas for the parallel configuration the charge is mainly stored in the crystal volume.

Considering the z -cut configuration, the PV current generates a charge accumulation at the two crystal surfaces (negative/positive charge at the $+c/-c$ faces). In a simple model,^[41] the charge accumulates only in the illuminated regions and the kinetics of accumulation at the $+c/-c$ faces can be described by:

$$\sigma = \sigma_{\infty} [1 - \exp(-t/\tau)] \quad (2)$$

with

$$\tau^{-1} = \frac{\mu e}{\varepsilon \varepsilon_0} n = \frac{\mu e}{\varepsilon \varepsilon_0} \frac{s\phi(x, y)[\text{Fe}^{2+}]}{\gamma[\text{Fe}^{3+}]}, \quad \sigma_{\infty} = \mp \frac{\varepsilon \varepsilon_0 l_{pv} \gamma[\text{Fe}^{3+}]}{e\mu} \quad (3)$$

μ being the electron mobility, n the electronic carrier concentration, ε the involved relative permittivity component of LiNbO_3 ($\varepsilon_{33} = 29.1$), ε_0 the vacuum permittivity, γ the trapping coefficient at Fe^{3+} impurities and $[\text{Fe}^{3+}]$ the concentration of acceptors. Note that the speed of the process, given by τ^{-1} , is linear with ϕ and so, with the light intensity I . The minus/plus sign in Equation 3 applies to the charge accumulated at the $+c/-c$ faces, respectively. This

charge density generates a bulk electric field which at steady-state conditions can be written as:

$$E_{pv} = \frac{j_{pv}}{en\mu} = \frac{l_{pv}\gamma[\text{Fe}^{3+}]}{\mu} \quad (4)$$

Although this model neglects transversal electron transport, it is a first approximation that allows gaining a useful physical insight into the PV effect features. It is worthwhile noting that in the case of non-uniform illumination $I(x,y)$, the time needed to reach the steady state is a function of the position, through $I(x,y)^{-1}$ (see Equation 3). That is the case for Gaussian illumination, used in this work, wherein the time constant τ increases with the distance to the spot center.

The PV evanescent fields generated in the substrate induce electrical forces on particles close to the surface. Electrically charged particles undergo electrophoretic forces ($\mathbf{f}_{ep} = q\mathbf{E}$), whereas neutral particles become polarized by the field and undergo dielectrophoretic forces.^[45] The latter ones can be written as:

$$\mathbf{f}_{ep} = -\bar{\nabla}(-\mathbf{p} \cdot \mathbf{E}) \quad (5)$$

\mathbf{p} being the dipole moment of the particle induced by the evanescent field \mathbf{E} .

These forces allow the manipulation and trapping of micro and nano-objects and are the basis for PVOT. The PV fields and so, the particle patterns, persist over a long time that depends on the dark conductivity of the crystal substrate, i.e. on the doping level and oxidation-reduction state ($[\text{Fe}^{2+}]/[\text{Fe}^{3+}]$). Typical times are in the range of minutes-months.^[17] Note that as the PV fields persist in the substrate in the dark, PVOT can operate illuminating previously or simultaneously to particle manipulation.

3. Results

3.1. Static Gaussian Beam Illumination

3.1.1. Simultaneous Experiments

Dynamic experiments reported in this section are essentially different from those described in previous work, that mostly use a sequential strategy for illumination and trapping. In the present case experiments follow a simultaneous procedure, i.e. particle deposition and illumination are carried out at the same time and observed in real time. We will see that this method gives rise to remarkable differences with respect to the experiments using sequential illumination and throws new light on the physics of the deposition and trapping of the particles.

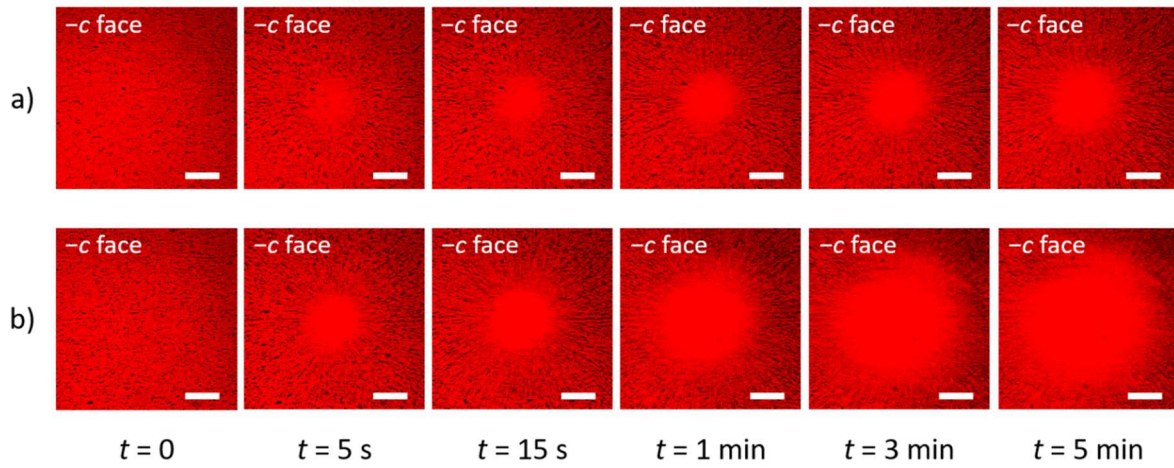


Figure 1. Microphotographs of the particle patterns obtained by the simultaneous method using a 16 μm -diameter Gaussian light spot, for different exposure times indicated in the figure and an average light intensity of a) 53 W cm^{-2} and b) 530 W cm^{-2} . Scale bar: 100 μm .

For the experiments we have used a static focused Gaussian beam with a diameter of $D = 4\sigma = 16 \mu\text{m}$ (where σ is the standard deviation of the Gaussian distribution) illuminating the $-c$ crystal face. The particle dynamics is illustrated in **Figure 1**, where photographs of the generated particle pattern at five increasing illumination times are shown for two different average light intensities of $I = 53 \text{ W cm}^{-2}$ (Figure 1a) and $I = 530 \text{ W cm}^{-2}$ (Figure 1b). The corresponding PV time response constant are 30 and 3 ms, respectively. Note, that this implies that in the scale of seconds shown in Figure 1 the PV fields are saturated in the center of the beam. For the case with $I = 530 \text{ W cm}^{-2}$ (Figure 1b), a fragment of the original video can be

found in the Supporting Information (Video S1).

One can see that the pattern evolves similarly with time for both light intensities although the effects are more pronounced for the highest I . At $t = 0$ prior to illumination, particles are homogeneously distributed on the substrate simply by gravity. During illumination, particles at the center of the spot progressively disappear and generate a well-defined circular region empty of particles surrounded by a wider, densely populated area, where radial dielectrophoretic chains can be distinguished. The diameter of the empty circle increases with time and it is considerably larger for the highest intensity.

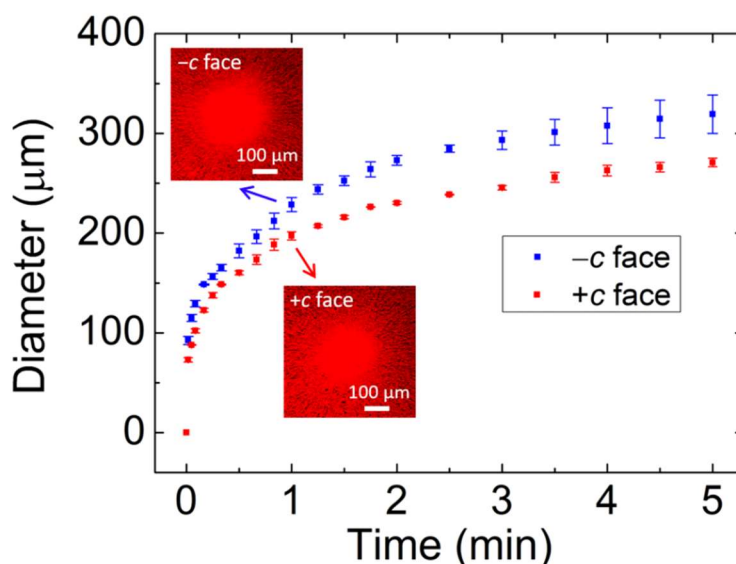


Figure 2. Time evolution of the diameter of the empty circle produced by a Gaussian light spot with diameter $4\sigma = 16 \mu\text{m}$ and average intensity $I = 530 \text{ W cm}^{-2}$ illuminating the $+c$ and $-c$ substrate faces using the simultaneous method.

These experiments have been repeated on the $+c$ face and similar results are obtained although the diameter of the empty circle is slightly smaller for this face. The dependence of the diameter of the empty circle on the illumination time for both crystal faces is plotted in **Figure 2** for $I = 530 \text{ W cm}^{-2}$. The curve shows a very rapid initial increase that slows down and nearly saturates at long times. This behaviour is probably related with the spatial dependence of the photovoltaic response with the distance to the center of the gaussian beam

discussed in section 2. In summary, during illumination, particles appear to be repelled and ejected from the region of the substrate that is illuminated with high intensity, whereas they become trapped at longer distances L from the center ($L \gg 4\sigma$). These results are surprising since, for the sequential method, particles get trapped in the illuminated regions, i.e. they behave oppositely. Anyhow, it is worthwhile noting that no “sequential experiments” using specifically Gaussian beam illumination on z -cut substrates have been reported yet. Therefore, we have also addressed sequential experiments in our setup to compare with our real-time (“simultaneous”) results.

3.1.2. Sequential and Hybrid Experiments

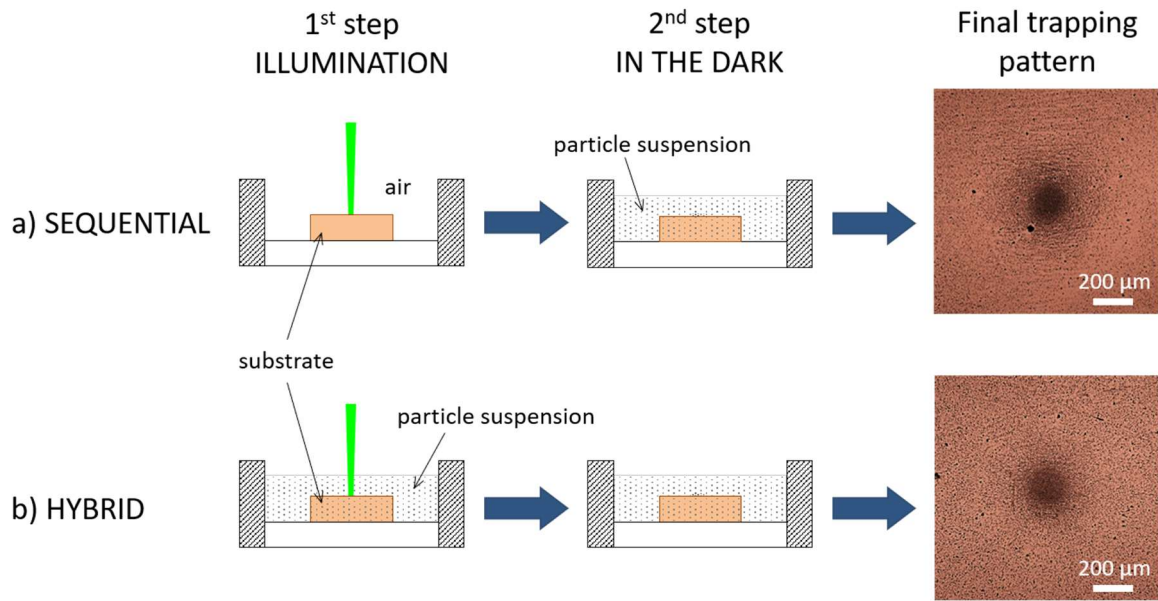


Figure 3. Microphotographs of the final particle patterns obtained for an illumination time of 10 s and intensity $I = 530 \text{ W cm}^{-2}$ using a) the sequential and b) the hybrid methods. See text.

For comparison with the above results, we have performed two kinds of experiments. The first kind consists of ordinary sequential experiments, using the method reported in the literature.^[19,23,25,41] The second type, which we will call hybrid experiments, combine a first step where particles are manipulated under illumination and a second step in the dark (see **Figure 3**). In the two cases the Gaussian beam is focused on the $-c$ face of the z -cut substrate,

which is the one in contact with the particle suspension.

In ordinary sequential experiments, the substrate is first illuminated with the focused laser beam during a time Δt either in air or in heptane and it is subsequently immersed for 3 min in the particle suspension allowing particle deposition (see Section 5). In Figure 3a, we show an illustrative result of the final particle pattern for an illumination time of $\Delta t = 10$ s and intensity $I = 530 \text{ W cm}^{-2}$. As expected from the previous reported data for the sequential method, particles are trapped on the illuminated region. However, the comparison between this sequential pattern with the simultaneous ones of Section 3.1.1 highlights the surprising different behaviour of the simultaneous experiments, in which we have observed for the first time particle ejection from the illuminated region with PVOT.

In hybrid experiments, we first perform a real-time experiment, as in Section 3.1.1, with an illumination time Δt followed by a period of time in the dark of 3 min. The substrate is inside the particle suspension during the whole experiment, i.e. under light exposure and in the dark. As in previous experiments, particle ejection from the center of the illuminated spot is observed during illumination, whereas particle deposition occurs in this area when the light is removed. An image of the final particle pattern obtained for the same illumination time and intensity as in the sequential experiment of Figure 3a is shown in Figure 3b. Consequently, in hybrid experiments, the data confirm that particle deposition occurs after illumination and the final pattern is roughly similar to the one for the sequential method.

3.2. From Trapping to Untrapping of Particles by Light Switching

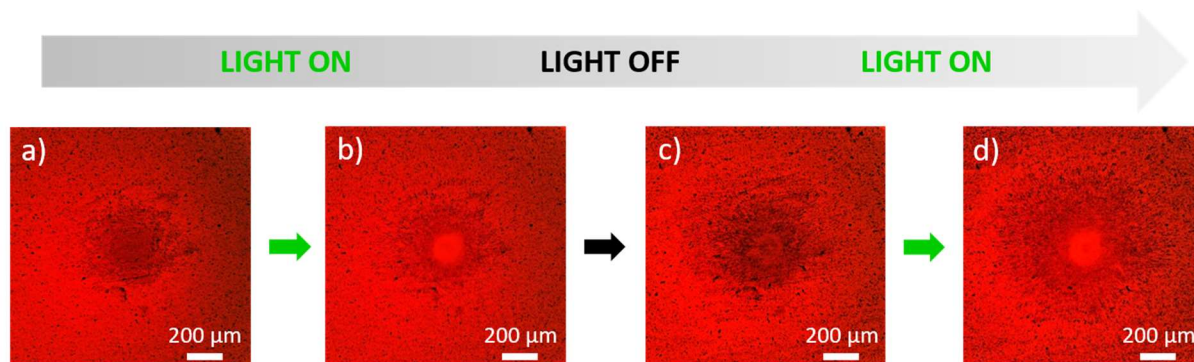


Figure 4. Microphotographs of the consecutive patterns obtained by switching on and off the exciting light ($I = 530 \text{ W cm}^{-2}$): a) Initial situation showing a pattern of deposited particles, b) pattern after illuminating the substrate for 40 s, c) pattern of trapped particles recovered in the dark and d) pattern after illuminating the substrate a second time for 140 s.

The experiments described above offer new possibilities for the application of PVOT. They provide a simple method to trap and untrap particles at will in the region illuminated with high intensity by successively switching the light off and on. Light on induces untrapping, whereas light off produces particle trapping again. The result for two cycles on the $-c$ face is shown in **Figure 4**. Considering the pattern of Figure 4a as starting point, when light is turned on particles are ejected from the center of the illuminated region and generate an empty area as shown in Figure 4b. When light is switched off, particles trap again in this region giving rise to the pattern of Figure 4c, similar to that of Figure 4a. Finally, after resuming the illumination we recover the empty region as can be seen in Figure 4d. This experiment demonstrates that the repulsion mechanism is able to remove the particles even when they are attached to the substrate by the attractive dielectrophoretic PV forces. This behavior provides a route for pattern or trap reconfiguration. This concept will be extended in the next Section by using moving light beams. In particular, we will see that, by conveniently moving the light beam, particles can be effectively removed from the selected trapping areas.

3.3. Moving Gaussian Light Beam

3.3.1. Patterns Formed by Empty or Filled Tracks

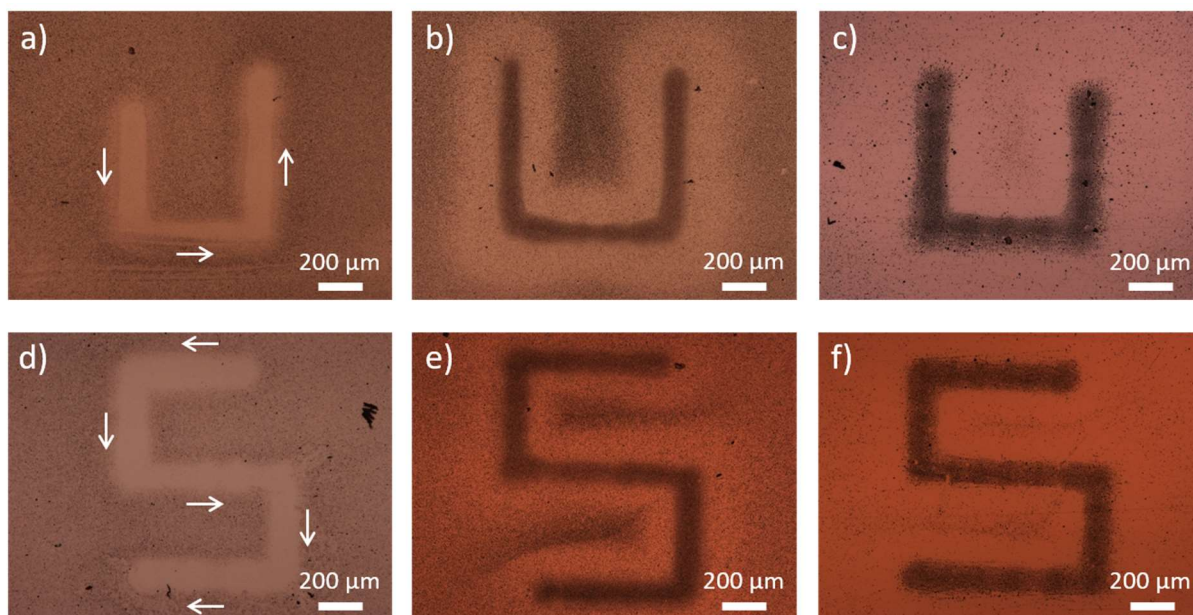


Figure 5. Images showing particle manipulation for a moving light spot drawing different trajectories as it is indicated by white arrows in a) and d). During illumination the substrate is in contact with a suspension with: a) and d) very low concentration of particles, and b) and e) very high concentration of particles. See text. Sequential experiments (illumination before particle manipulation) with the same light trajectory are shown in c) and f). Patterns a), b) and c) have been generated on the $-c$ face, whereas d), e) and f) correspond to the $+c$ face.

To our knowledge, PVOT experiments with a moving light spot, even using a sequential procedure, have not been reported so far. Hence, we have addressed this kind of experiments by displacing the Gaussian light spot along the substrate surface of a z -cut $\text{LiNbO}_3\text{:Fe}$ sample. The light intensity in all cases is 530 W cm^{-2} . For the simultaneous method, as it could be expected from the results of Figure 1, the moving spot generates a track free of particles on the substrate surface initially covered with an homogeneous background of deposited particles. The results can be seen in **Figure 5a** and **5d** for two different light paths (for more details, see Video S2 in the Supporting Information). Then, after drawing the desired trajectory with the beam, the resulting empty track can be refilled and a trapping track is generated if there are enough particles in the suspension, as shown in Figure 5b and 5e (hybrid experiments). The untrapping and trapping processes that have allowed the generation of empty and filled tracks should have the same origin to that of experiments with static Gaussian beam which also exhibit repulsion or re-trapping for the simultaneous (Figure 1) or hybrid methods (Figure 3b),

respectively. Finally, since sequential experiments with moving Gaussian beams have not been addressed so far, Figure 5c and 5f presents the corresponding sequential experiments in which illumination is performed in heptane but particles are added right after light is turned off (see Video S3 in the Supporting Information). Well defined trapping patterns following the light trajectory are observed, showing that moving light beam is another useful strategy to draw particle patterns. The microphotographs shown in Figure 5 are taken after carefully removing the substrate from the suspension to obtain better images with a Nikon microscope. Additional experiments with a variety of light paths have been successfully carried out showing that arbitrary tracks are easily recorded.

3.3.2. Pattern Erasure and Reconfiguration

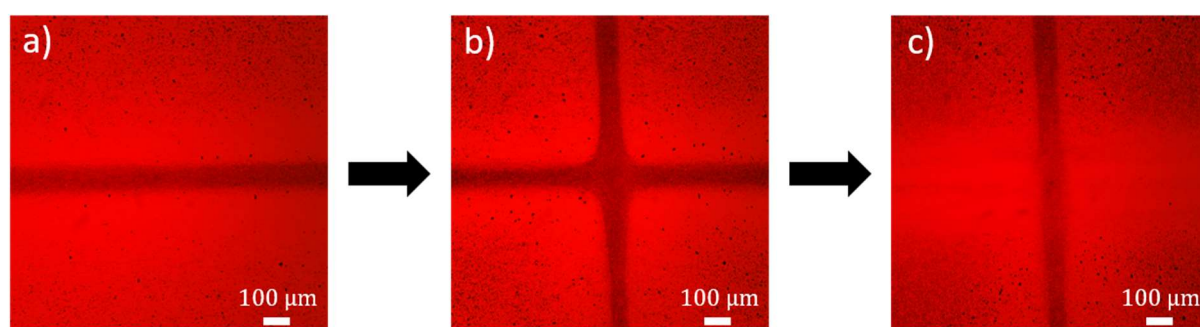


Figure 6. Images showing a sequence of three patterns. The second and third ones are obtained by reconfiguration of the previous patterns. a) Horizontal particle track obtained by a sequential experiment with moving Gaussian beam ($I = 530 \text{ W cm}^{-2}$). b) Modified pattern after sequentially adding a new vertical track ($I = 530 \text{ W cm}^{-2}$). c) Final pattern generated by erasing the initial horizontal track in a simultaneous experiment ($I = 1060 \text{ W cm}^{-2}$).

Combining particle ejection by simultaneous operation with particle trapping by the sequential or hybrid methods, flexible erasure and reconfiguration of patterns become possible. To illustrate this novel function of PVOT, a sequence of three patterns obtained on the $-c$ face by applying the reconfiguration capabilities are shown in **Figure 6**. In Figure 6a a photograph of a horizontal particle fringe is presented, which has been recorded by using the sequential method with a moving light beam. A second pattern consisting in a cross is

obtained by additionally recording a vertical track (see Figure 6b) using the same method as in Figure 6a. Finally, in order to obtain the last pattern (see Figure 6c), we take advantage of the erasure functionality of real-time illumination (as shown in Video S4, Supporting Information). By scanning the light beam across some convenient regions of the horizontal fringe, one can remove particles keeping only the vertical fringe shown in Figure 6c.

4. Discussion and Conclusions

A systematic experimental study to investigate the simultaneous method, i.e. real-time operation of PVOT, has been developed and the results have been compared to those obtained with the generally used two-step sequential method. Since PV fields remain in the sample after illumination, the latter method was preferred in previous work in order to simplify the experimental setup. Using static Gaussian beam illumination on *z*-cut LiNbO₃:Fe substrates, remarkable unexpected differences between these two methods have been observed. The sequential method induces particle trapping in the illuminated area, whereas the simultaneous method causes particle repulsion. This repulsion occurs in both polar faces, $+c$ and $-c$, and the diameter of the empty region increases with light intensity and with the illumination time (see Figure 2). The novel repulsion phenomenon cannot be described with previous theory on PVOT, which predicts PV-field induced dielectrophoretic trapping of neutral metal particles in the illuminated region.^[42,43]

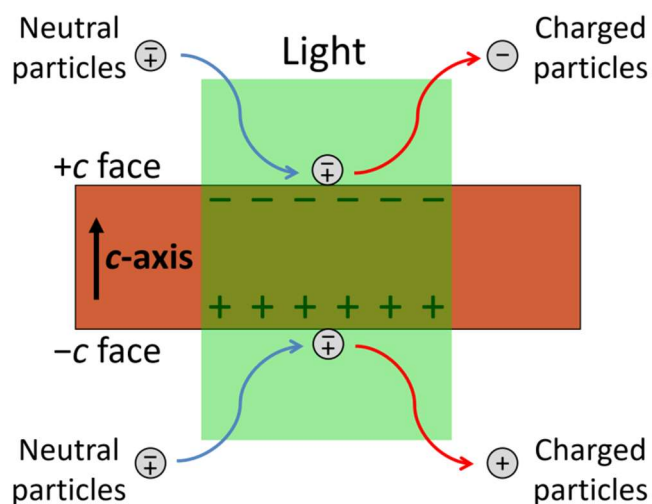


Figure 7. Schematic diagram of the proposed mechanism for particle ejection based on charge exchange between the nanoparticles and the LiNbO₃:Fe z-cut substrate under illumination.

To explain that new particle ejection phenomenon we advance here a possible mechanism consisting of charge exchange between the LiNbO₃ sample and the metallic particles for both +*c* and −*c* faces. The process is schematically illustrated in **Figure 7**. Under illumination, particles approaching the substrate become charged after being in contact with the crystal surface. Once particles are charged with the same sign as the surface, they are repelled by electrophoretic, instead of dielectrophoretic forces. Note that under illumination, due to the PV effect, light can recharge the crystal surface maintaining the charging process.

A quite similar transfer process between nanoparticles and the LiNbO₃:Fe substrate has been already proposed in an early paper using PV particle trapping in other experimental conditions (*y*-cut substrates under sinusoidal illumination).^[39] In addition, other charge transfer phenomena have been already observed on undoped LiNbO₃ surfaces such as reduction of Ag⁺ ions from AgNO₃ solutions.^[46] Anyhow, further work will be necessary to investigate in depth and to confirm this proposal.

The repulsion phenomenon, not reported for other optoelectronic platforms, has suggested additional manipulation possibilities that have been explored. In the case of a moving light

spot, the repulsion effect allows removing the particles along the beam path generating an empty trajectory. However, when light is turned off, particles can be trapped again if they are still available in the suspension. Note that the results with moving light are consistent with the physical picture proposed for static experiments. Additionally, our results have suggested an alternative procedure to address illumination in sequential experiments, not used so far: the PV field can be also recorded by drawing a light pattern using a moving light beam. The

In summary, from the technological point of view, the new experiments offer a new remarkable capability to PVOT, light-induced repulsion of particles from the substrate, that can be combined with trapping effects. This provides additional functionalities for particle manipulation and patterning, such as pattern drawing (based on trajectories either empty or filled with particles along the light spot path), and erasure and reconfiguration of particle structures. Other interesting possibilities like massive charging of particles can be envisaged, in comparison to other optical techniques. Moreover, the new functionalities appear well suited to be implemented in optofluidic devices that can be built on the PV substrates as already proposed in references.^[21,47] All these technological capabilities remarkably enhance the potential and versatility of PVOT promising interesting new developments in the near future.

5. Experimental Section

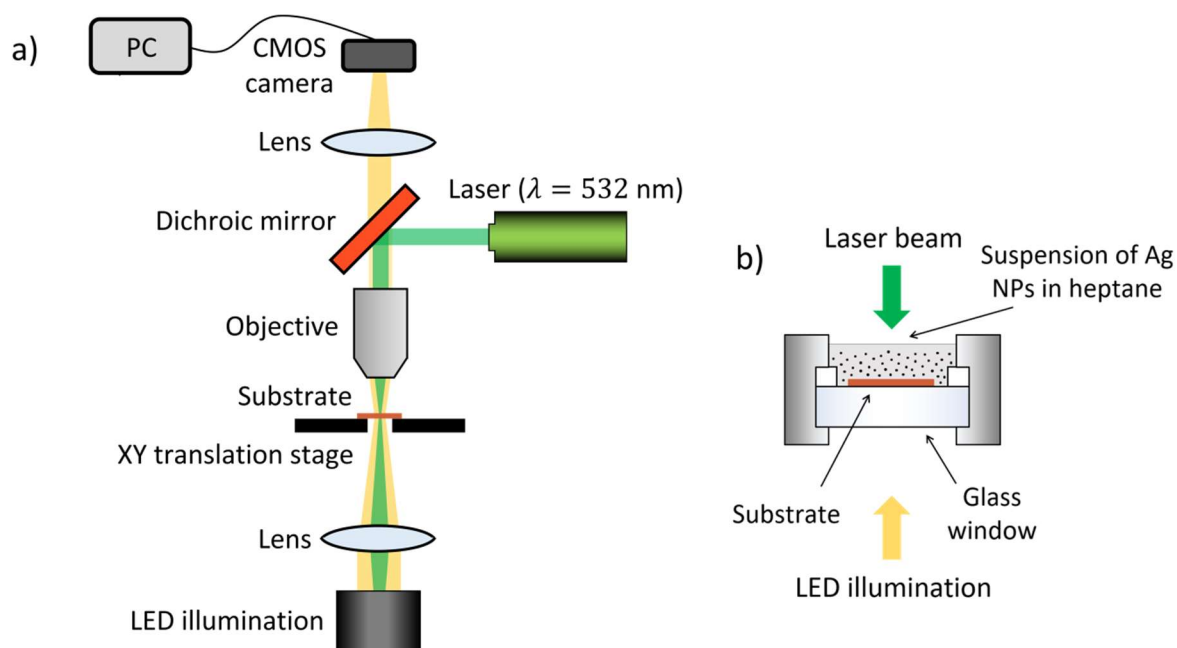


Figure 8. a) Schematic representation of the experimental setup. b) Detailed view of the open cuvette containing the PV substrate in contact with a suspension of NPs for manipulation.

Experimental setup: An illustration of the experimental setup can be found in **Figure 8a**. It simultaneously enables real-time particle manipulation by PVOT as well as visualization. As PV substrate, highly doped z-cut $\text{LiNbO}_3\text{:Fe}$ plates (0.25 mol%) were used, with thicknesses of 0.5 mm and 1 mm (purchased from Hangzhou Freqcontrol Electronic Technology Ltd.). A frequency-doubled Nd:YAG laser operating at 532 nm was used in order to generate the PV effect in the $\text{LiNbO}_3\text{:Fe}$ substrate, whereas a white-light LED lamp was used for visualization. The laser beam was focused on the surface of the substrate by means of a microscope objective (Mitutoyo) with 20X magnification and numerical aperture $NA = 0.42$, although other objectives were available for observation purposes. The diameter of the focused Gaussian beam at the focal plane ($4\sigma = 16 \mu\text{m}$) was measured with an optical beam profiler (Model NS2-SI/9/5-PRO, Ophir Optonics). Intensities ranging from 53 W cm^{-2} to 1.06 kW cm^{-2} were used (the power of the beam was determined with a photodiode and the average intensity was calculated as $I = P/\pi(2\sigma)^2$, where P is the power of the beam). The intensity of the LED lamp was always kept lower than $80 \mu\text{W cm}^{-2}$ to ensure that it did not produce any

significant additional PV effect in the crystal in the time scale of the experiments presented in this work. The PV crystal was placed on top of an XY translation stage that can be manually moved in two dimensions, thus changing the position of the substrate with respect to the beam spot and enabling experiments with a moving Gaussian beam. In order to monitor the experiments and acquire real-time footage, a CMOS camera was employed (Model DFK MKU130-10x22, The Imaging Source). Additionally, as the final particle patterns obtained by PVOT remain stable after illumination, photographs with better quality could also be taken with a Nikon microscope after carefully taking the crystal out of the particle suspension.

Deposition methods: For massive trapping and manipulation, suspensions of spherical Ag nanoparticles in heptane were prepared (average diameter $d = 100$ nm, purchased from Skyspring Nanomaterials, Inc.). In all experiments the NP concentration in the suspension was 50 mg L^{-1} except for the experiment of Figure 6, in which the concentration was 500 mg L^{-1} . The sample was placed inside an open cuvette in contact with the suspension so that particles could be trapped and manipulated on the upper surface of the PV substrate (see Figure 8b). Three different deposition methods were employed and compared:

- Sequential method. First, the substrate was illuminated, giving rise to a PV electric field distribution. This initial step can be carried out either in air or in heptane. Then, the cuvette was filled with NP suspension. Finally, the crystal was left in contact with the suspension in the dark, producing the corresponding particle pattern on its surface.
- Simultaneous method. The cuvette was first filled with NP suspension and then the substrate was illuminated in contact with the suspension. Therefore, generation of the PV electric field and particle manipulation occur at the same time.
- Hybrid method. Analogously to the simultaneous method, the cuvette was first filled with NP suspension and the substrate was illuminated afterwards. However, in hybrid experiments the crystal was subsequently left in the dark, as in sequential experiments.

Supporting Information

Supporting Information is available from the Wiley Online Library or from the author.

Acknowledgements

Financial support from Ministerio de Ciencia, Innovación y Universidades of Spain (MAT2014-57704-C3, MAT2017-83951-R) is gratefully acknowledged. Carlos Sebastián also acknowledges Institute of Materials Science Nicolás Cabrera for the Research Award for Physics Students 2018.

Received: ((will be filled in by the editorial staff))

Revised: ((will be filled in by the editorial staff))

Published online: ((will be filled in by the editorial staff))

References

- [1] D. G. Grier, *Nature* **2003**, 424, 810.
- [2] D. Psaltis, S. R. Quake, C. Yang, *Nature* **2006**, 442, 381.
- [3] M. Maragò, P. H. Jones, P. G. Gucciardi, G. Volpe, A. C. Ferrari, *Nat. Nanotech.* **2013**, 8, 807.
- [4] P. Rodríguez-Sevilla, L. Labrador-Páez, D. Jaque, P. Haro-González, *J. Mat. Chem. B* **2017**, 5, 9085.
- [5] A. Ashkin, *Phy. Rev. Lett.* **1970**, 24, 156.
- [6] A. Ashkin, J. M. Dziedzic, J. E. Bjorkholm, S. Chu, *Opt. Lett.* **1986**, 11, 288.
- [7] M. P. MacDonald, G. C. Spalding, K. Dholakia, *Nature* **2003**, 426, 421.
- [8] M. Woerdemann, C. Alpmann, M. Esseling, C. Denz, *Laser Photonics Rev.* **2010**, 22, 4176.
- [9] M. L. Juan, M. Righini, R. Quidant, *Nat. Photonics* **2011**, 5, 349.
- [10] P. Y. Chiou, A. T. Ohta, M. C. Wu, *Nature* **2005**, 436, 370.
- [11] A. Jamshidi, P. J. Pauzauskie, P. J. Schuck, A. T. Ohta, P. Y. Chiu, J. Chiu, P. Yang, M. C. Wu, *Nat. Photonics* **2008**, 2, 86.

- [12] M. C. Wu, *Nat. Photonics* **2011**, *5*, 322.
- [13] S. Zhang, N. Shakiba, Y. Chen, Y. Zhang, P. Tian, J. Singh, M. D. Chamberlain, M. Satkauskas, A. G. Flood, N. P. Kherani, S. Yu, P. W. Zandstra, A. R. Wheeler, *Small* **2018**, *14*, 1803342.
- [14] J. Villarroel, H. Burgos, A. García-Cabañes, M. Carrascosa, A. Blázquez-Castro, F. Agulló-López, *Opt. Express* **2011**, *19*, 24320.
- [15] H. A. Eggert, F. Y. Kuhnert, K. Buse, J. R. Adleman, D. Psaltis, *Appl. Phys. Lett.* **2007**, *90*, 241909.
- [16] M. Esseling, *Photorefractive optoelectronic tweezers and their applications*, Springer, Heidelberg, Germany **2015**.
- [17] M. Carrascosa, A. García-Cabañes, M. Jubera, J. B. Ramiro, F. Agulló-López, *Appl. Phys. Rev.* **2015**, *2*, 040605.
- [18] E. M. De Miguel, J. Limeres, M. Carrascosa, L. Arizmendi, *J. Opt. Soc. Am. B* **2000**, *17*, 1440.
- [19] J. F. Muñoz-Martínez, M. Jubera, J. Matarrubia, A. García-Cabañes, F. Agulló-López, M. Carrascosa, *Opt. Lett.* **2016**, *41*, 432.
- [20] M. Esseling, A. Zaltron, C. Sada, C. Denz, *Appl. Phys. Lett.* **2013**, *103*, 061115.
- [21] L. Miccio, P. Memmolo, S. Grilli, P. Ferraro, *Lab Chip* **2012**, *12*, 4449.
- [22] I. Elvira, J. F. Muñoz-Martínez, M. Jubera, A. García-Cabañes, J. L. Bella, P. Haro-González, M. A. Díaz-García, F. Agulló-López, M. Carrascosa, *Adv. Mater. Technol.* **2017**, *2*, 1700024.
- [23] I. Elvira, J. F. Muñoz-Martínez, A. Barroso, C. Denz, J. B. Ramiro, A. García-Cabañes, F. Agulló-López, M. Carrascosa, *Opt. Lett.* **2018**, *43*, 30.

- [24] A. Blázquez-Castro, J. C. Stockert, B. López-Arias, A. Juarranz, F. Agulló-López, A. García-Cabañes, M. Carrascosa, *Photochem. Photobiol. Sci.* **2011**, *10*, 956.
- [25] M. Jubera, I. Elvira, A. García-Cabañes, J. L. Bella, M. Carrascosa, *Appl. Phys. Lett.* **2016**, *108*, 023703.
- [26] L. Miccio, V. Marchesano, M. Mugnano, S. Grilli, P. Ferraro, *Opt. and Lasers in Eng.* **2016**, *76*, 34.
- [27] M. Esseling, A. Zaltron, W. Horn, C. Denz, *Laser and Photonics Rev.* **2015**, *9*, 98.
- [28] L. Chen, S. Li, B. Fan, W. Yan, D. Wang, L. Shi, H. Chen, D. Ban, S. Sun, *Scientific Reports* **2016**, *6*, 29166.
- [29] B. Fan, F. Li, L. Chen, L. Shi, W. Yan, Y. Zhang, S. Li, X. Wang, X. Wang, H. Chen, *Phys. Rev. Appl.* **2017**, *7*, 064010.
- [30] K. Buse, *Appl. Phys. B* **1997**, *64*, 273.
- [31] F. Agulló-López, G. F. Calvo, M. Carrascosa, In *Photorefractive Materials and Their Applications I* (Eds: P. Günter, J. P. Huignard), Springer, New York, USA **2006**, Ch. 3.
- [32] P. Ferraro, S. Grilli, L. Miccio, V. Vespini, *Appl. Phys. Lett.* **2008**, *92*, 213107.
- [33] S. Grilli, P. Ferraro, *Appl. Phys. Lett.* **2008**, *92*, 239202.
- [34] S. Grilli, S. Coppola, G. Nasti, V. Vespini, G. Gentile, V. Ambrogio, C. Carfagna, P. Ferraro, *RSC Adv.* **2014**, *4*, 2851.
- [35] G. Nasti, S. Coppola, F. Olivieri, V. Vespini, V. Pagliarulo, P. Ferraro, *Langmuir* **2018**, *34*, 2198.
- [36] A. Puerto, J. F. Muñoz-Martín, A. Méndez, L. Arizmendi, A. García-Cabañes, F. Agulló-López, M. Carrascosa, *Opt. Express* **2019**, *27*, 804.
- [37] A. García-Cabañes, A. Blázquez-Castro, L. Arizmendi, F. Agulló-López, M. Carrascosa,

Crystals **2018**, *8*, 65.

[38] A. Blázquez-Castro, A. García-Cabañes, M. Carrascosa, *Appl. Phys. Rev.* **2018**, *5*, 041101.

[39] X. Zhang, J. Wang, B. Tang, X. Tan, R. A. Rupp, L. Pan, Y. Kong, Q. Sun, J. Xu, *Opt. Express* **2009**, *17*, 9981.

[40] S. Glaesener, M. Esseling, C. Denz, *Opt. Lett.* **2012**, *37*, 3744.

[41] J. F. Muñoz-Martínez, I. Elvira, M. Jubera, A. García-Cabañes, J. B. Ramiro, C. Arregui, M. Carrascosa, *Opt. Mater. Express* **2015**, *5*, 1137.

[42] C. Arregui, J. B. Ramiro, A. Alcázar, A. Méndez, J. F. Muñoz-Martínez, M. Carrascosa, *J. Eur. Opt. Soc.* **2015**, *10*, 15026.

[43] J. F. Muñoz-Martínez, J. B. Ramiro, A. Alcázar, A. García-Cabañes, M. Carrascosa, *Phys Rev. Appl.* **2017**, *7*, 064027.

[44] B. Sturmann, V. Fridkin, *Photovoltaic and Photorefractive effects in noncentrosymmetric materials*, Gordon and Breach Science Publishers, Philadelphia, USA **1992**.

[45] T. B. Jones, *Electromechanics of particles*, Cambridge University Press, Cambridge, UK **1995**.

[46] Y. Sun, B. Eller, R. Nemanich, *J. Appl. Phys.* **2011**, *110*, 084303.

[47] M. Esseling, F. Holtmann, M. Woerdemann, C. Denz, *Opt. Express* **2010**, *18*, 17404.

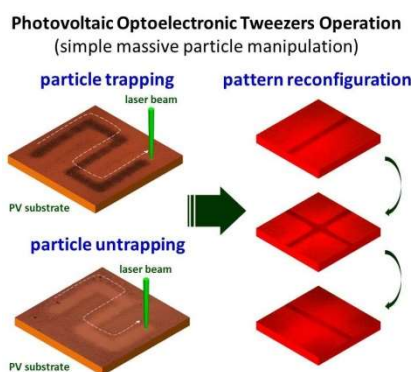
New optoelectronic strategies for massive nanoobject manipulation and reconfigurable patterning are demonstrated. All novel functionalities are based on the singular photoelectric properties of $\text{LiNbO}_3\text{:Fe}$ that include high photoinduced electric fields and effective interaction between the nanoobjects and the ferroelectric surface. Thereby, it is proved that this material is an outstanding substrate that remarkably enhances the capabilities of photovoltaic optoelectronic tweezers.

Keyword

E. Muñoz-Cortés, A. García-Cabañes, M. Carrascosa*

Real-Time Operation of Photovoltaic Optoelectronic Tweezers: New Strategies for Massive Nanoobject Manipulation and Reconfigurable Patterning

ToC figure



Supporting Information

Real-Time Operation of Photovoltaic Optoelectronic Tweezers: New Strategies for Massive Nanoobject Manipulation and Reconfigurable Patterning

*Carlos Sebastián-Vicente, Esmeralda Muñoz-Cortés, Angel García-Cabañes, Fernando Agulló-López, and Mercedes Carrascosa**

Video S1. Fragment of the simultaneous experiment corresponding to Figure 1b, which illustrates particle untrapping when light ($I = 530 \text{ W cm}^{-2}$) is turned on. The position of the light spot is indicated by a white dot at the center. The timer at the top shows the actual time scale of the experiment.

Video S2. Real-time monitoring of the experiment of Figure 5d, showing the generation of a track empty of particles along the light path using a moving Gaussian beam ($I = 530 \text{ W cm}^{-2}$). The position of the light spot is indicated by a white dot at the center. The timer at the top shows the actual time scale of the experiment.

Video S3. Video showing the steps involved in the trapping procedure of a sequential experiment. First, the substrate is illuminated with a moving Gaussian beam ($I = 530 \text{ W cm}^{-2}$) following a specific path (indicated in the video with a white dashed line at the time $t = 33 \text{ s}$). In this step, the substrate surface is in contact with heptane (without particles). Then, particles are added with a pipette and they rapidly get trapped along the path previously followed by the Gaussian beam. The position of the light spot is indicated by a white dot at the center. The timer at the top shows the actual time scale of the experiment.

Video S4. Erasure of a previously generated particle pattern, enabling the transition from Figure 6b to Figure 6c (reconfiguration). The position of the light spot ($I = 1060 \text{ W cm}^{-2}$) is indicated by a white dot at the center. The timer at the top shows the actual time scale of the experiment.